Primljen / Received: 4.5.2024.
Ispravljen / Corrected: 18.9.2024.
Prihvaćen / Accepted: 5.10.2024.
Dostupno online / Available online: 10.12.2024.

Fatigue characterisation of concrete composite girder with steel bottom plate and corrugated web under uniform corrosion environment

Authors:

Prof. **Genhui Wang**, PhD. CE
Lanzhou Jiaotong University, Lanzhou, China
Department of Civil Engineering
13609341991@139.com

Pulu Han, PhD. CE
Lanzhou Jiaotong University, Lanzhou, China
Department of Civil Engineering
465267760@qq.com
Corresponding author

Assoc.Prof. **Xuejun Jin**, PhD. CE
Lanzhou Jiaotong University, Lanzhou, China
Department of Civil Engineering
184929439@QQ.com

Research Paper

Genhui Wang, Pulu Han, Xuejun Jin

Fatigue characterisation of concrete composite girder with steel bottom plate and corrugated web under uniform corrosion environment

The objective of this study was to elucidate the fatigue characteristics of a concrete composite girder with a steel bottom plate and a corrugated web (Hereinafter referred to as CGSBCW), and compute its bending moment of inertia under uniform corrosion conditions by incorporating the corrosion rate parameter in the calculations. The corrosion rate was, in turn, determined from the stress value measured in the test. The stress amplitude – fatigue life (S–N) equation of the CGSBCW under uniform corrosion conditions was derived using the Paris semi-empirical law and Lemaitre fatigue life calculation formula. The Lemaitre parameters of the CGSBCW were determined through theoretical calculations and numerical simulations. The relationship among the stress amplitude, fatigue life, and corrosion rate when the corrosion rate was less than 20% was numerically fitted. Curvatures for the stress amplitude, fatigue life, and corrosion rate were confirmed. The results demonstrated that salt-corrosive environment had a significant impact on the fatigue characteristics of composite girders. For the same level of loading, it increased the stress amplitude and decreased the fatigue life. At a corrosion rate of 9%, the stresses in the test girders increased by 10%, while the fatigue life decreased by 24.5%. When the corrosion rate was less than 20%, the stress amplitude and fatigue life, respectively, increased and decreased essentially linearly with the increase in corrosion rate.

Key words:
uniform corrosion, corrugated steel web girder, corrosion rate, stress amplitude, fatigue life

Prethodno priopćenje

Genhui Wang, Pulu Han, Xuejun Jin

Značajke zamora betonskoga spregnutog nosača s čeličnom donjom pločom i valovitim hrptom u jednolikome korozivnom okolišu

Cilj ovog istraživanja bio je razjasniti značajke zamora betonskog spregnutog nosača s čeličnom donjom pločom i valovitom hrptom (u daljnjemu tekstu: CGSBCW) i izračunati njegov moment inercije pri savijanju pod jednolikim korozivnim uvjetima uključivanjem parametra brzine korozije u izračune. Brzina korozije određena je na temelju vrijednosti naprezanja izmjerene u ispitivanju. Jednadžba amplitude naprezanja – otpornosti na zamor (S–N) CGSBCW-a pod jednolikim korozivnim uvjetima izvedena je primjenom Parisova poluempirijskog zakona i Lemaitreove formule za izračun otpornosti na zamor. Lemaitreovi parametri CGSBCW-a određeni su teorijskim izračunima i numeričkim simulacijama. Odnos između amplitude naprezanja, otpornosti na zamor i brzine korozije, kada je brzina korozije manja od 20 %, postavljen je numerički. Potvrđene su zakrivljenosti za amplitudu naprezanja, otpornost na zamor i brzinu korozije. Rezultati su pokazali da solni korozivni okoliš ima znatan utjecaj na značajke zamora spregnutih nosača. Za istu razinu opterećenja povećana je amplituda naprezanja i smanjena otpornost na zamor. Pri brzini korozije od 9 % naprezanja u ispitnim nosačima porasla su za 10 %, dok se otpornost na zamor smanjila za 24,5 %. Kada je brzina korozije bila manja od 20 %, amplituda naprezanja i otpornost na zamor povećavali su se i smanjivali uglavnom linearno s povećanjem brzine korozije.

Ključne riječi:
jednolika korozija, valoviti čelični hrbat, brzina korozije, amplituda naprezanja, otpornost na zamor

1. Introduction

Corrugated steel web girder bridges have the advantages of light weight and high prestressing efficiency and can effectively solve structural problems caused by thermal stresses and shrinkage, creep, and other factors [1-4]. In recent years, this girder structure has emerged prominently in the field of bridge construction. The use of reinforced concrete slabs as the bottom plate in conventional corrugated steel web girders presents problems, such as easy cracking of the bottom plate when subjected to positive moments [5]. A study by Idiart [6] showed that in salt-aggressive environments, such as offshore structures, cracks accelerate the ingress of corrosive ions, which seriously affects the life of the girder.

To solve this problem, researchers in China have opted to use flat steel plates instead of concrete bottom plates used in traditional composite girders. Problems, such as cracks and corrosive ion intrusion in concrete bottom plates can be resolved using flat steel plates instead of concrete bottom plates, as they provide the advantages of both the concrete top plate's compression resistance and steel bottom plate's tensile resistance to the composite structure. This is achieved by reducing the weight of the structure and improving its spanning capacity. Furthermore, they are versatile and easy to use.

Consequently, girders are being increasingly used. However, only a few studies have been conducted on the fatigue performance of this type of girders, including the fatigue of the welded joints in this new design. Particularly, studies on the fatigue properties of these girders when subjected to corrosion have been scarce. The focus of current research on the fatigue performance of corrugated steel web composite girders is on traditional corrugated steel web composite girder bridges [7]. Although the fatigue properties of such concrete composite girders with steel bottom plates and corrugated webs (Hereinafter referred to as CGSBCW) have been studied [12-15], the influence of corrosive environment has not been analysed. Researchers have adopted the notch stress [16] and structural stress [17] methods to analyse the fatigue performance of girder and summarised the corresponding fatigue damage prediction models [18]. In [19] the fatigue performance of this new type of composite girders under a corrosive environment was examined. However, none of these studies elaborated on the specific connection between the corrosion rate and variables, such as stress amplitude (S) and fatigue life (N).

To address the aforementioned gaps In this study, the stress amplitude of CGSBCW under a uniform corrosion condition was first calculated by incorporating the corrosion rate parameter (η_s) into the moment of inertia. Subsequently, relying on Paris' semi-empirical rule and Lemaitre's fatigue life equation, the S–N curve formulae of the CGSBCW under a uniform corrosion environment was derived, and the fatigue life parameters of the CGSBCW were determined via model testing and numerical simulation. Finally, S and N of the CGSBCW under uniform corrosion conditions were analysed by numerical fitting method. The relationship curves of η_s with S and N were determined. Thus, this study serves as a basis and reference for the design optimisation, theory and calculation methodology, and application promotion of CGSBCW bridges.

2. Theoretical foundation

2.1. Momentum of corrosion

During forceful deformation of the corrugated web, the contraction of the corrugated form replaces the elastic deformation of the flat steel plate in a way analogous to an 'accordion'. This effect is known as the 'fold effect'. According to results of recent research [4], when calculating the bending stiffness of a girder section with corrugated webs, the top and bottom plates satisfy the flat cross-section assumption, and the contribution of the corrugated webs to the bending stiffness is ignored, i.e. it satisfies the 'quasi-plane assumption'. The moment of inertia of the composite girder in a corrosive environment can be estimated by calculating it by assuming that the top concrete section is equivalent to a steel plate section:

$$I_f = \sum_{i=1}^{2}\left(\frac{b_i h_{fi}^3}{12} + b_i e_{fi}^2 h_{fi}\right) \tag{1}$$

where I_f is the bending moment of inertia of the girder in the corrosive environment [mm^4]; I is the number of plates composing the girder (the bottom plate is numbered 1, while the top plate is numbered as 2); e_{fi} is the coordinate of the centre of form of the cross section of each plate [mm]; h_{fi} is the vertical height of the cross section of each plate [mm]; and b_i is the width of each plate [mm].

Because chloride ions are the primary corrosive ions in a corrosive environment, the impact of chloride salts on the concrete top slab can be disregarded. The weight loss of the girder after corrosion is due mainly to the reduction of the vertical height h of the steel bottom plate (i.e., the thickness of the plate), and η_s of the steel can be defined by the "rate of loss of thickness".

$$\eta_s = \frac{m_0 - m_s}{m_0} = \frac{h_w - h_f}{h_w} \tag{2}$$

When η_s from Eq. (2) is introduced and expanded, I_f of the composite girder in a corrosive environment can be determined as

$$I_f = \frac{b_1 h_{w1}\left(1-\eta_s\right)^3}{12} + b_1 h_{w1}\left(1-\eta_s\right)e_{f1}^2 + \frac{b_2 h_2}{12} + b_2 h_2 e_{f2}^2 \tag{3}$$

where h_w is the thickness of the steel plate before corrosion [mm].

2.2. Stress amplitude (S)

As per the relevant norms [22], fatigue loading calculations require S to be multiplied by an extra amplification factor, in

cases where S is defined as the difference between the highest and lowest stresses. According to the mechanics of materials, S of a girder loaded at three points can be calculated using the following formula:

$$S_r = (1+\Delta\varphi)(\sigma_{Mf} - \sigma_{mf}) = (1+\Delta\varphi)\frac{(F_M - F_m)Ly}{4I_f} \quad (4)$$

where Δφ is the amplification factor; σ_M and σ_m are the maximum and minimum stresses; F_M and F_m are the maximum and minimum loads; L is the calculated span of the girder body; and y is the vertical coordinates of the section.

2.3. Fatigue life (N)

Continuous damage mechanics theory can be utilised to calculate N of a material or structure. The calculation of N in the Lemaitre damage model [22] is dependent on the maximum and minimum stresses, and is expressed as

$$N = \frac{(\beta+1)(\sigma_M^{\beta+1} - \sigma_m^{\beta+1})^{-1}}{2BR_c^{S_0}(\beta+2)} \quad (5)$$

where $\beta = 2S_0 + m - 1$, $B = m/(2ES_1)^{S0}K^m$, and $R_c = 2(1+\nu)/3 + 3(1-2\nu)(\sigma_m/\sigma_{eq})^2$. . Here, K, m, S_0 and B and B are the material parameters; R_c is the stress triaxiality, and $R_c = 1$ in the one-dimensional case; and D is the damage variable.
The value of N of the composite girder can be determined using the stress-amplitude calculation method as

$$N_f = \frac{(\beta+1)\left[\left((1+\Delta\varphi)\frac{F_M Ly}{4I_f}\right)^{\beta+1} - \left((1+\Delta\varphi)\frac{F_m Ly}{4I_f}\right)^{\beta+1}\right]^{-1}}{2BR_c^{S_0}(\beta+2)} \quad (6)$$

2.4. S–N curve

Paris proposed a semi-empirical law [23], which is currently the most widely used research method for S–N curves. In double logarithmic form, S–N curves are frequently expressed as follows:

$$\log N = \log p - m\log S \quad (7)$$

where m and p are material parameters.
By combining Eqs. (3), (5), and (6), the S–N curve of the composite girder in a corrosive environment is obtained as follows:

$$\log\frac{(\alpha+1)\left[\left((1+\Delta\varphi)\frac{F_M Ly}{4I_f}\right)^{\alpha+1} - \left((1+\Delta\varphi)\frac{F_m Ly}{4I_f}\right)^{\alpha+1}\right]^{-1}}{2BR_c^{S_0}(\alpha+2)} = \quad (8)$$
$$= \log p - m\log\left[(1+\Delta\varphi)\frac{(F_M - F_m)Ly}{4I_f}\right]$$

Where je $I_f = \frac{b_1 h_{w1}(1-\eta_s)^3}{12} + b_1 h_{w1}(1-\eta_s)e_{f1}^2 + \frac{b_2 h_2}{12} + b_2 h_2 e_{f2}^2$,

and the reduction in the thickness of the bottom plate, is primarily reflected in the calculation of the moment of inertia.

3. Model test

3.1. Material and dimensional parameters

Two pieces of the composite girder were designed and fabricated in a reduced-scale model as follows: The top slab and diaphragm were made of C50 [22] concrete, of which the top slab was 1000 mm wide and 50 mm thick; the end diaphragm was 150 mm thick; and the centre diaphragm was 100 mm thick. Both the web and bottom plate were made of Q345 steel [22]; the web plate was made of a corrugated steel plate, rolled and moulded in a factory with a thickness of 3 mm, and the bottom plate was made of a flat steel plate with a width of 580 mm and a thickness of 5 mm. The girder model had a span L of 3.4 m, calculated span L_0 of 3.2 m, and girder height h of 400 mm. The bottom plate girder end was simply supported, with five diaphragms located at the pivot point, L/4, and mid-span section. Figures 1, 2, and 3 depict the cross-sectional dimensions, corrugated steel web, and embedded connectors, respectively.

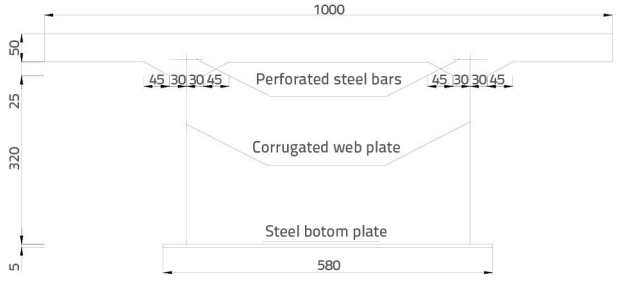

Figure 1. Cross-sectional dimensions for the geometric model (unit: mm)

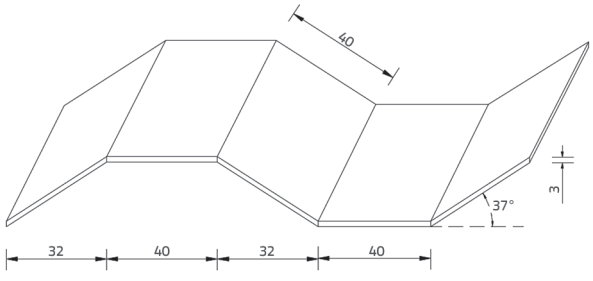

Figure 2. Unit ripple size of web plate (unit: mm)

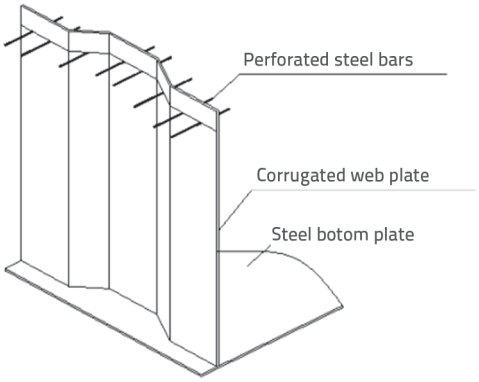

Figure 3. Schematic of shear connection parts

3.2. Salt corrosion test

In a corrosive environment, the girder is generally surrounded by corrosive air, which is equivalent to immersion. To accelerate the test process, a salt corrosion test was conducted using a long-term immersion method, in which the girders were fully immersed.

Compared with the immersed steel, the immersed concrete had a higher concentration of salt solution during the salt corrosion test. Owing to the corrosive effects of concrete, the diffusion of salt ions was necessary. Steel was directly exposed to corrosive ions, resulting in galvanic corrosion. Compared with the corrosion results, there was a delay in the corrosion results for concrete. This was to determine if this delay would affect the structure's utilization. Based on the research findings from the chlorine salt erosion test over the years, the immersion time for the salt corrosion test was set to 18 months.

The girder was formed by combining steel and concrete, and long-term immersion tests can be accelerated by increasing the solution's concentration. Hence, the concentration of NaCl solution was chosen to be 6% for this test. As depicted in Figure 4, one of the test girders was immersed in the NaCl solution and designated as girder #2, whereas, the unimmersed test girder was designated as girder #1.

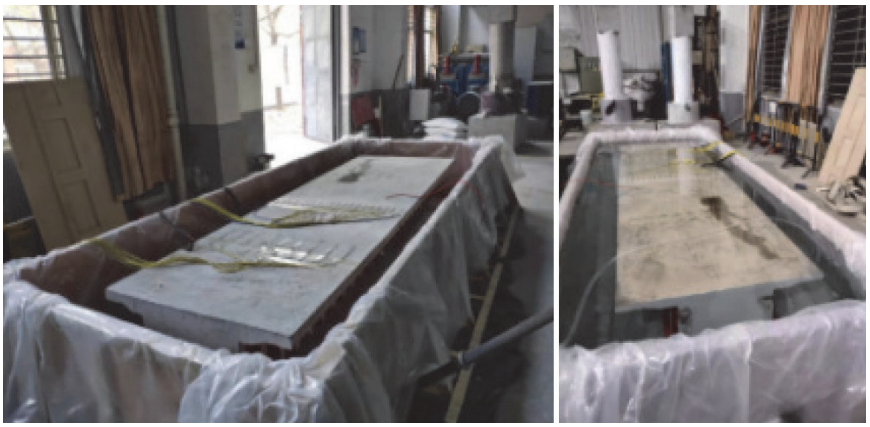

Figure 4. Girder corrosion test setup

3.3. Test girder loading

Both the test girders underwent fatigue and static tests under the same load rating. Two types of fatigue loading tests were reported [22], which include the fatigue characteristic test and fatigue failure test. Sinusoidal fatigue loads were utilised, and the load frequency was determined to be 3 Hz. The fatigue load calculation model from [21] was used to calculate the fatigue loads of the original bridge. Using the constant load stress value as the lower limit for loading the composite girder model, the stress value when working with constant load was assumed and the live load on the girder model was considered as the upper limit value. For 2 million cycles, the fatigue test load was subjected to loads with upper and lower limits of 53.5 and 16.5 kN, respectively. The fatigue failure test exhibited an increase in load amplitude and a graded result.

Table 1. Load stages for fatigue failure test

Load rating	Median load [kN]	Load magnitude [kN]	Number of cycles (×10 000)
1	40	48	40
2	49	64	40
3	57	82	40
4	64	98	40
5	72	114	40
6	80	128	40
7	86	144	30
8	90	160	20
9	96	176	20
10	100	192	slom

Table 1 lists the loading conditions and Figure 5 shows the fatigue loads. Static loading was followed by each level of the fatigue-loading cycle, which had a maximum load of 80 kN. Test data were collected at every 10 kN after static loading.

3.4. Measurement points for test girder

Figure 6 shows the placement and naming of the strain gauges in the middle portion of the test girder.

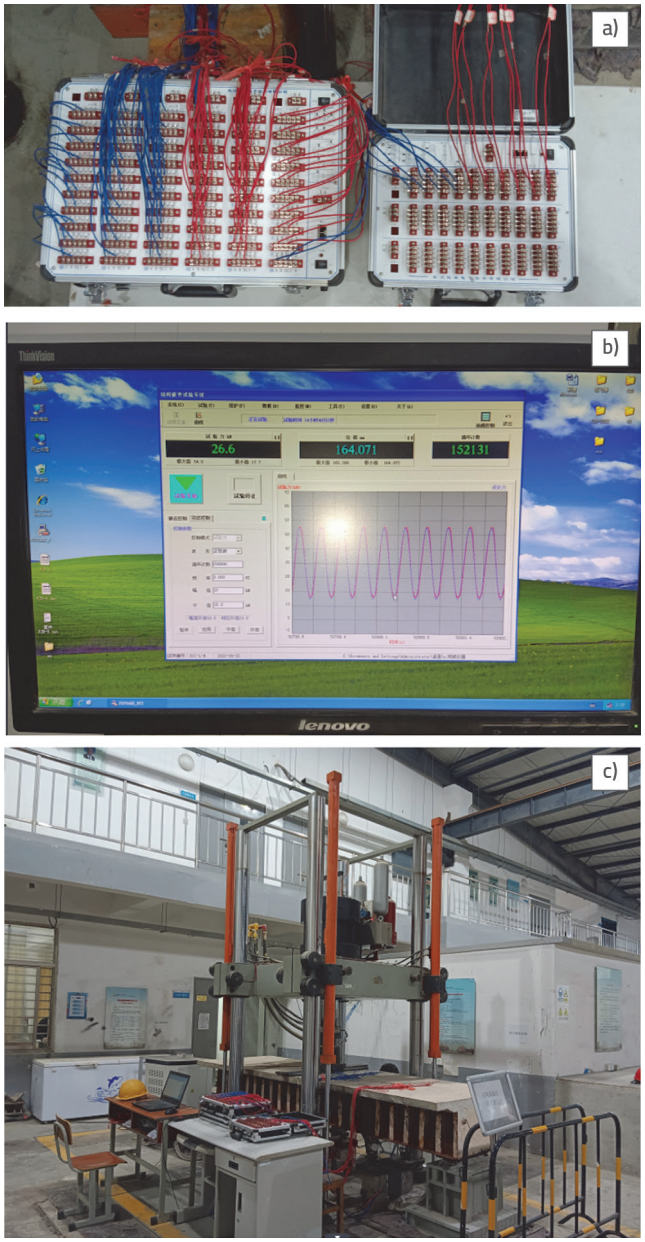

Figure 5. Girder fatigue test: a) Stress–strain sampling system, b) Fatigue loading system, c) Test girder loading

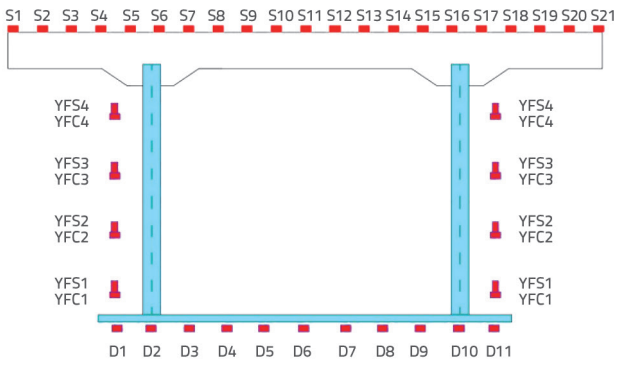

Figure 6. Layout of strain gauges across the fracture surface

4. Numerical simulation

The numerical simulation process comprises two main steps [25], as enumerated below: The solid model of the test girder was created using the Abaqus finite element software for numerical modelling. Next, the numerical results were imported into the 'Fe-safe' fatigue calculation software is for fatigue calculation.

4.1. Creation of girder components

To construct the concrete and steel bottom plates, cross-sectional parameters, including the width and height of the girder, were utilised, as shown in Figure 1. The corrugated form steel parameters shown in Figure 2 were used to construct the steel webs. Concrete and steel plates were simulated by C3D8R units, while the reinforcement was served by T3D2 units.

4.2. Numerical modelling of connectors

The connections shown in Figure 3 were used to construct the connectors. 'Embedded region' facilitated the connection of the reinforcement to the concrete top slab. To start with, the 'Embedded region' method involves burying the connecting reinforcement into the concrete top slab. 'Coupling' refers to the connection between the connecting bars and corrugated web. Holes were drilled in the concrete section of the corrugated web at appropriate locations To complete attaching the corrugated web to the top plate, the holes were connected to the midpoints of the reinforcement using the ''Coupling' method. The girder had a total of 284 connections on either side. This is shown in Figure 7.

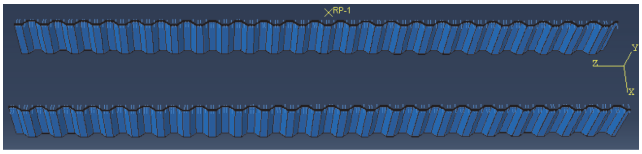

Figure 7. Connector models

4.3. Assembly of corrugated web and bottom plate

The binding constraints link the corrugated web to the steel bottom plate. The numerical simulation model of the beam is shown in Figure 8.

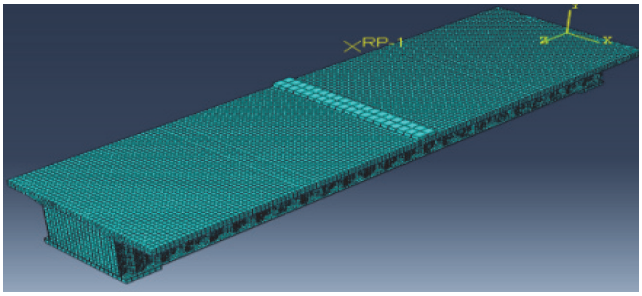

Figure 8. Finite element model of the experimental girder

4.4. Corrosion of girders

By altering the thickness of the bottom plate, the corrosion results of the girders were obtained using the calculation principle laid out in Eq. (2). The amount of thickness change was back-calculated using Eq. (3) and relevant theory of material mechanics, based on the test results.

4.5. Fatigue analysis of girder body

The fatigue analysis of the girder was performed using 'Fe-safe' software, and the steps involved are as follows [25]:

- The model was established using 'Abaqus' software and static calculations were performed on the model. Based on the test loading conditions, a minimum load amplitude (16.5 kN) was selected as the loading value.
- The Abaqus results were imported into Fe-Safe for fatigue calculation.
- Next, a computing group was chosen in Fe-safe; the components of the fatigue calculation were identified, based on the test results, which were the corrugated web and steel bottom plate.
- Subsequently, the material parameters were established. The appropriate material parameters from were chosen from the software material library and assigned to the appropriate parts.
- Subsequently, the load spectrum was established. Loads were added in multiples, i.e., by selecting the load minimum, load median, load maximum in the load magnitude. The load spectrum was established based on the relationship between the loads applied during the static calculations and multiples of the minimum value of the load, the median value of the load, and the maximum value of the load.
- Fatigue calculations were then performed by selecting parameters, such as N in the desired calculation results. This location was selected to save the calculation results. The results of the calculations can be opened and viewed in Abaqus.

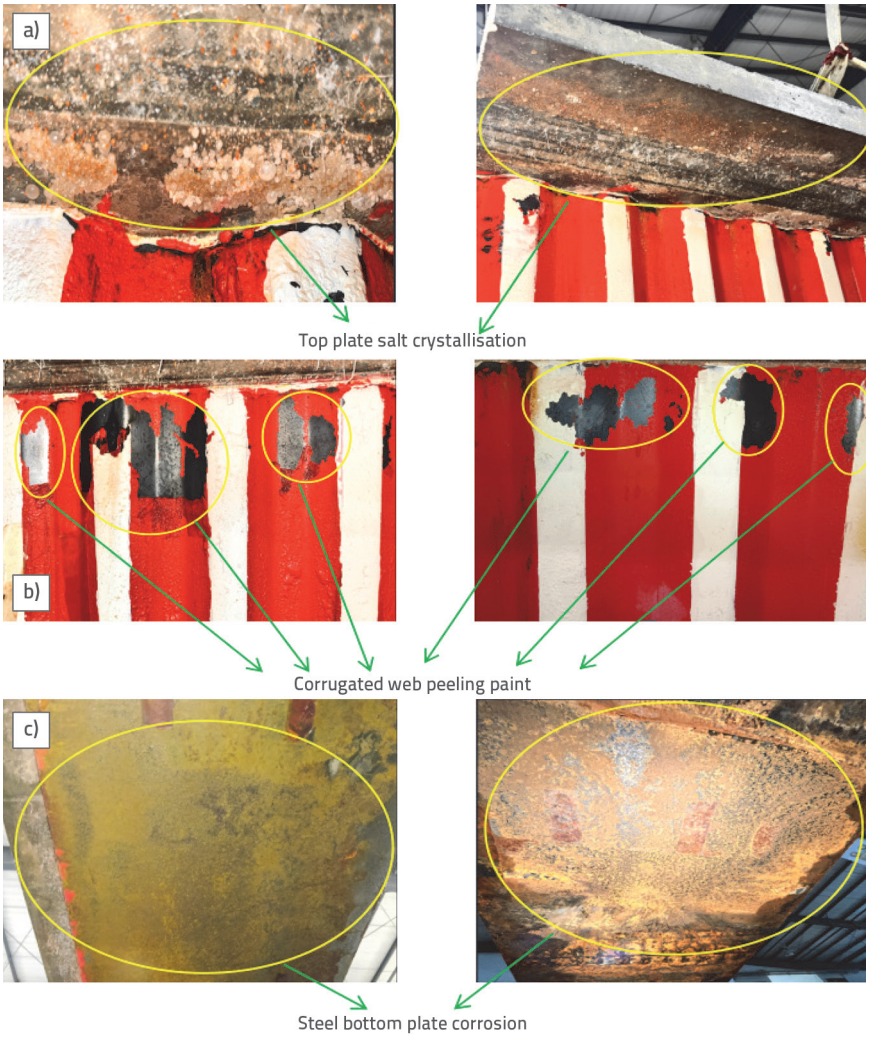

Figure 9. Surface of the girder after the corrosion test: a) Top plate salt crystallisation; b) Corrugated web with corroded and peeling paint; c) Bottom plate corrosion

5. Analysis and discussion of results

5.1. Corrosion phenomenon analysis

Figure 9 depicts the appearance of test girder #2 after corrosion. After corrosion, the test girders exhibited salt crystallisation on the top plate, corrosion and peeling of paint on the web, and rust on the bottom plate. Because salt crystallisation in the top slab was not severe, the corrosive effect of chloride salts on the concrete could be ignored. Because of the protective effect of the coating layer, corrosion did not have a significant effect on the steel web. However, significant corrosion was observed on the bottom plates, which were the focus of the post-corrosion test girder performance analysis.

Because of the concrete protection, no corrosion occurred on the reinforcement in the top slab. As shown in Figure 10, the chloride ions can be ignored in the top plate of the composite girder.

5.2. Fatigue failure form analysis

Figure 11 shows the final failure of the test girder. Figure 11 shows that Test girder #1 suffered only one crack at the

Figure 10. Corrosion of steel bars

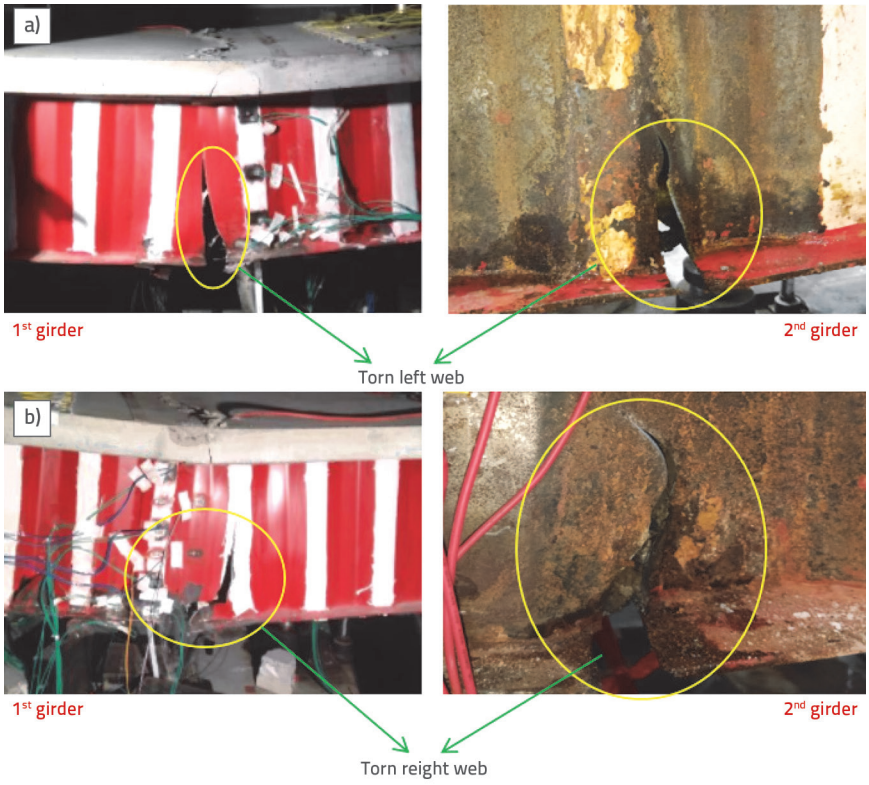

Figure 11. Test girder failure patterns: a) Left web crack; b) Right web crack

bottom. During the destruction of the test girder, the webs on the left and right sides were torn, resulting in cracks that progressed upward. Test girder #1 had a fatigue source at the weld point of the interface between the bottom and web plates. From the test results, it can be seen that the fatigue failure of the uncorroded test girder is the fatigue failure of the solder joint. The failure process was in line with the general law of fatigue failure of the weld joints. Failure of test girder #2 caused the webs on both sides to tear, similar to the failure behaviour of test girder #1. A crack formed upward along the girder cross-section. Fatigue failure was still present in the welded joints, with the fatigue source located at the interface between the bottom plate and web. The crack in test girder #2 remained near the middle section of the girder. This demonstrates that the uniform corrosion at the interface did not affect the weld, thus becoming a fatigue source for fatigue failure.

When the failure locations of the two test girders were compared, it could be observed that fatigue failure could be caused by the midspan cross-section of the girder. A uniform corrosion would not influence the weld to become a fatigue source for fatigue failure in the mid-span cross section, which is considered a hazardous cross section for the fatigue failure of girders.

5.3. Stress analysis before and after corrosion

At 80 kN, stress results were obtained using the adopted static test values. As an example of the results after 1 and 2 million cycles of fatigue loading, the stress values of the fatigue characterisation test are presented. As an example of the results after the aforementioned load cycles under 49 and 72 kN of fatigue loading, the stress values of the fatigue failure test are presented. These are illustrated in Figure 12.

As shown in Figure 14, Test girder #1 exhibited a lower stress level than test girder #2. After the corrosion, the stress levels increased by approximately 10%. Combining this result with the stress calculation formula for a three-point loaded girder would allow the calculation of parameters, such as the girder corrosion rate. As shown in Figure 14.a, after 1 and 2 million fatigue tests, the stress values of the two test girders were relatively similar. Corrosion reduced the effective bearing area of the test girders, whereas fatigue loading did not. As demonstrated in Figure 10.b: after the median load was applied after the number of load cycles under 49 and 72 kN fatigue loadings, the two test girders showed significant differences in their respective stress values. This indicated that the effective bearing area of the test girder decreased during the fatigue failure test. Calculations were necessary to determine the exact number of cycles that occurred.

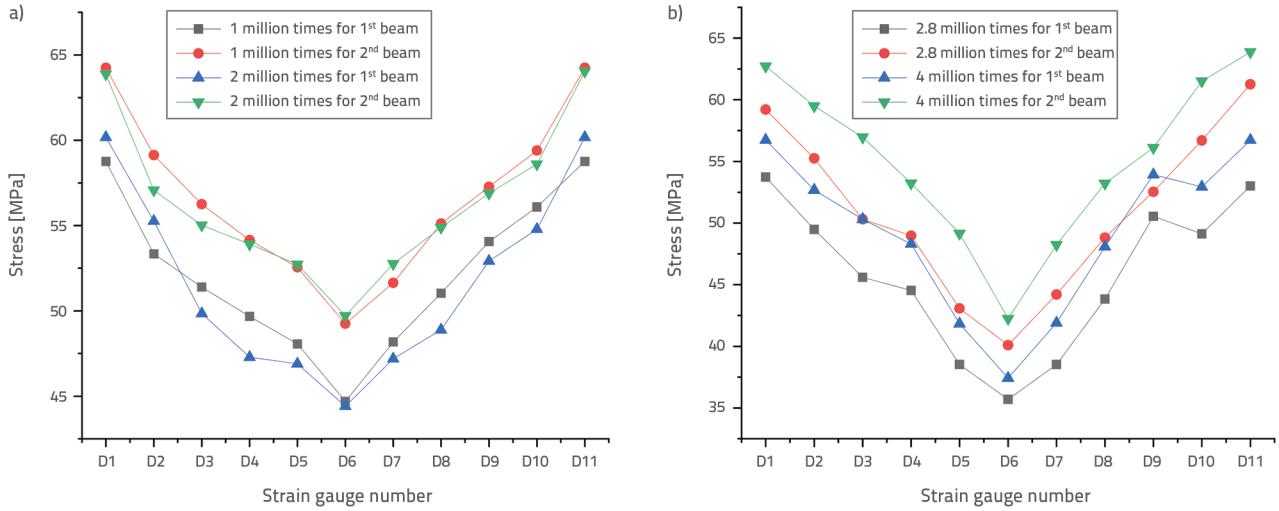

Figure 12. Bottom plate stress: a) Fatigue characteristic test stress; b) Fatigue failure test stress

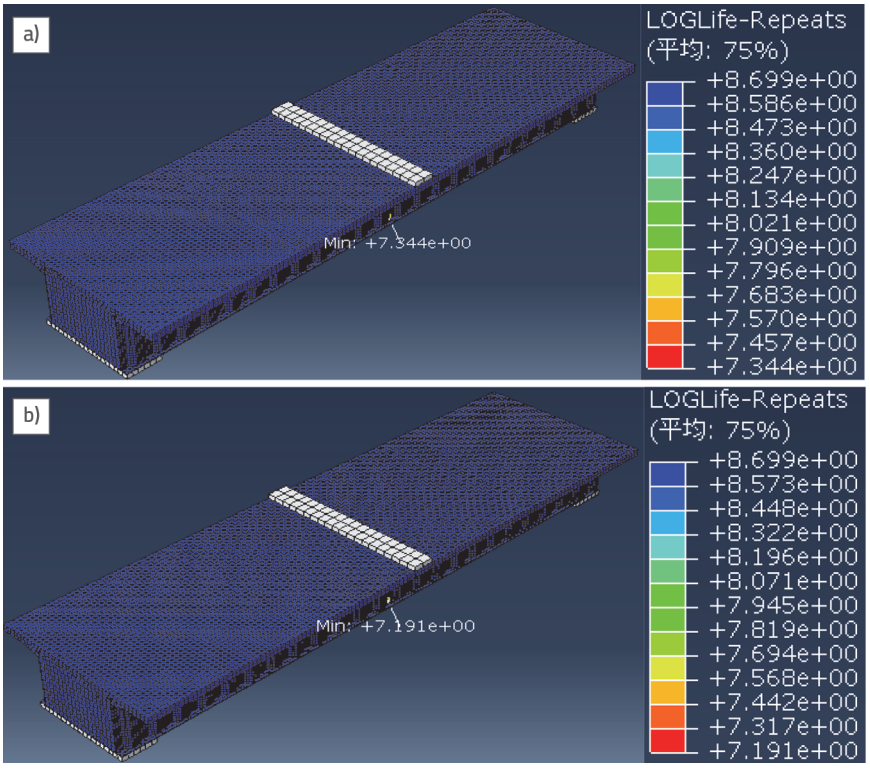

Figure 13. Cloud chart of simulated fatigue lives of test girders #1 and #2: a) Girder #1; b Girder #2

5.4. Corrosion rate of composite girders

It was observed from the test stress results that subsequent to corrosion, the test girders experienced an increase in the stress by approximately 10%. Combining Eqs. (2) and (3), and knowledge of material mechanics is necessary to obtain: The corrosion rate of the test girder is 9%, and the thickness of the corroded steel backing plate is 4.55 mm.

5.5. Fatigue life of composite girders

Figure 13 shows that the numerical simulation could validate the fatigue life calculation. Table 2 presents the results of the fatigue life calculations for girders #1 and #2.

Figure 15 and Table 2 reveal that the theoretical calculation model's accuracy would be indicated by the fact that the inaccuracies associated with the theoretical and simulated values were less than 5%. The test girders experienced a significantly shorter fatigue life after corrosion than before. Test girder #2 had a longer fatigue life than test girder #1 due to a 24.5% decrease in the rate of corrosion. Salt corrosion was proven to be highly detrimental to the fatigue life of the composite girders. Based on the results of the fatigue life calculations in the numerical simulations, the fatigue parameters β *B* and *Rc* of the composite girders were determined by back calculation using

Table 2. Fatigue resistance of the test beam

Test girder	Fatigue life		Inaccuracy [%]
	Theoretical value	Analog value	
1	21123995.1	22080047.3	4.5
2	15952654.0	15523870.1	2.7

Table 3. Load levels and fatigue life

Loading amplitude [kN]	**Stress amplitude S** [MPa]		**Fatigue life N** [ciklusi]	
	1	**2**	**1**	**2**
37	31.8	34.9	21123995.1	15952654.0
48	41.2	45.3	12189817.4	9205642.1
64	55.0	60.4	5989159.0	4522959.8
82	70.5	77.4	3371952.2	2546468.4
98	84.2	92.5	2198427.8	1660233.2
114	98.0	107.6	1478668.6	1116677.4
128	110.0	120.8	1064116.1	803611.1
144	123.7	135.9	805838.8	608562.3
160	137.5	151.0	647147.3	488720.0
176	151.2	166.1	510764.0	385724.4
192	165.0	181.2	422838.2	319323.7

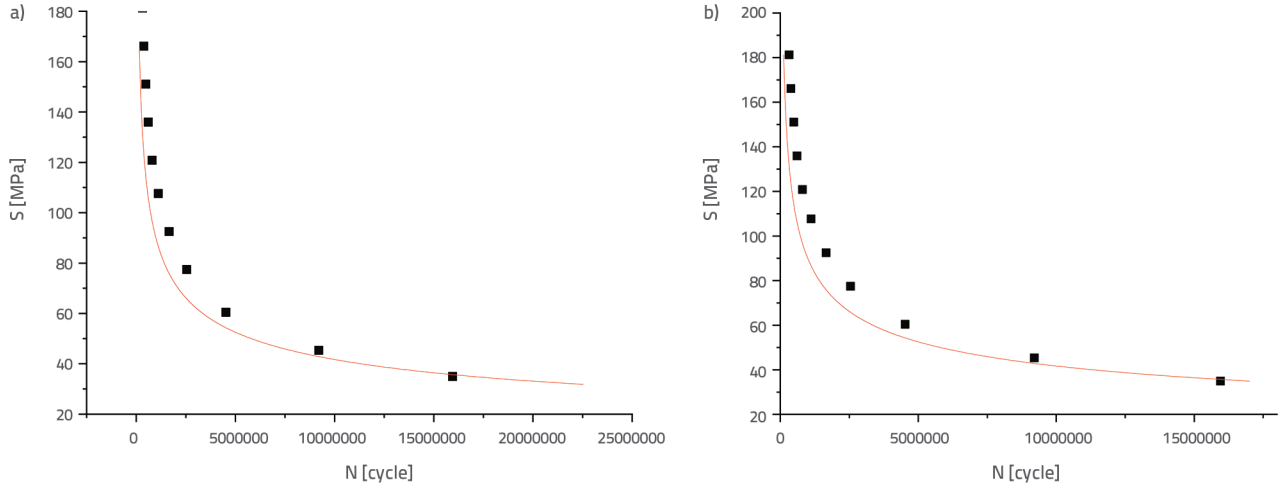

Figure 14. S–N curve of test girders: a) Girder 1; b) Girder 2

Eqs. (5) and (6), respectively. According to the test results, the steel bottom plate maintained a one-dimensional tensile state. Thus, R_c = 1 was obtained. Based on the calculations, β = 2.22 and $B = 1.962 \times 10^{-13}$.

5.6. S–N curves of composite girders

After determining the parameters β, B, and Rc, the fatigue life of the composite girder was calculated using Eq. (6). After applying the loading conditions listed in Table 1, the stress amplitude and fatigue life of the composite girders were calculated. The S–N curves of the composite girders were fitted and analysed. Table 3 displays the results of the stress amplitude and fatigue life calculations, inform which the S–N curves of the girder were fitted. Figure 14 shows the fitted S–N curves. Origin software was used to fit the data, and exponential form was used for the fitting equation. Next, the exponential equation was transformed by Eqs. (7) and (8), and the S–N curves in the logarithmic form were obtained. To represent the S–N curves of the composite girder, the logarithmic form with a value of 3 for the parameter m was used. The S–N curves for the composite girders before and after corrosion, had the following forms:
Before corrosion:

$$\log N_w = 11{,}8599 - 3\log S_w \quad (9)$$

After corrosion:

$$\log N_f = 11{,}8603 - 3\log S_f \quad (10)$$

Table 3 and Figure 16 demonstrate that girder #1 had an inferior S in the S–N curve than girder #2; yet girder #1 had a superior N. The value of N of the corroded test girders was reduced at the same stress level, as demonstrated in this study. Test girders that were not corroded could endure higher stresses, while maintaining the same N. This implies that corrosion led to an increase in S and a decrease in N of the S–N curves.
When the exponential parameter *m* in the S–N curve was fixed at 3, the fitted values of p before and after the corrosion were

Table 4. Stress amplitude and fatigue life at different corrosion rates

Corrosion rate η_s [%]	Stress amplitude		Fatigue life	
	S [MPa]	**Advance** [%]	**N** [ciklus]	**Reduction** [%]
0	31.8	0.00	21123995.1	0.0
1	32.1	1.0	20501494.6	3.0
2	32.4	2.0	19892011.6	5.8
3	32.8	3.1	19293417.0	8.7
5	33.4	5.2	18165305.8	14.0
7	34.2	7.5	17019859.9	19.4
9	34.9	9.9	15952654.0	24.5
12	36.1	13.6	14437920.4	31.7
15	37.4	17.6	13019908.9	38.4
20	39.7	24.9	10868430.8	48.6

p_{w1} = 7.24289×10^{11} and p_{w2} = 7.24905×10^{11}. A difference of 0.85 per thousand is negligible. A uniform corrosion had a major influence on the values taken for S and N, as evidenced by these results.

5.7. Discussion of results for different corrosion rates

Nine corrosion rates, as listed in Table 4, were selected to clarify the influence law of corrosion on stress amplitude and fatigue life of the test girders. A test load of 37 kN was used. Table 4, and Figures 15 and 16 reveal that when the corrosion rate was less than 20%, the stress amplitude and fatigue life, respectively, increased and decreased linearly with the corrosion rate. The relationships among the stress amplitude S, fatigue life N, and corrosion rate η_s were obtained as:

$$S = 31{,}602 \pm 0{,}390\ h_s \quad (11)$$

$$N = 2{,}087 \times 10^7 - 518461{,}803\ h_s \quad (12)$$

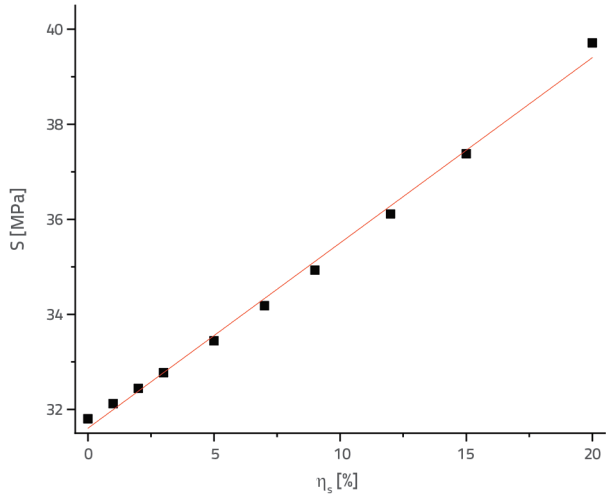

Figure 16. S–η_{ss} curve of the test girder

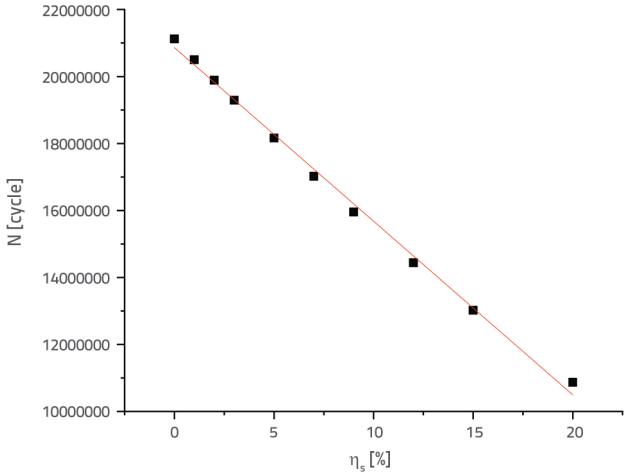

Figure 16. N–η_s curve of the test girder

6. Conclusion

Based on this analysis, the following conclusions were drawn.

- Uniform corrosion did not affect the fatigue failure mode of the girder body. Under uniform corrosion, the fatigue failure section of the girder body lay near the mid-span. The corrugated angle of the welding of the bottom plate and corrugated web played a role in determining the position of fatigue failure; the fatigue failure mode was caused by the fatigue failure of the solder joints.
- Uniform corrosion caused the effective bearing thickness of the test girder bottom to decrease, which increased the stress on the girder bottom and decreased its fatigue performance. According to the computed results, a reduction in the thickness of the bottom plate would cause a change in the moment of inertia of the girder. After 18 months of soaking in a 6% NaCl solution, the stress of the girder increased by approximately 10%, according to the test results. According to the theoretical calculations, the corrosion rate was 9%.

- Uniform corrosion decreased the fatigue life of the test girder, as determined from the analysis results. According to the numerical simulation and theoretical calculations, the fatigue life was reduced by 24.5% when the corrosion rate was 9% %. The salt corrosion environment was detrimental to the fatigue life of composite girders, as demonstrated by this study.
- Using numerical simulation and theoretical computations, the Lemaitre parameters, *Rc*, β, and *B* of the composite girder were determined to be 1, 2.22, and 1.962 $\times 10^{-13}$, respectively.
- The same were used to analyse the relationship among the corrosion rate, stress amplitude, and fatigue life. The results showed that when the corrosion rate of uniform corrosion was less than 20%, the stress amplitude increased linearly with the corrosion rate, while the fatigue life decreased linearly with the corrosion rate. The corrosion rate and stress Amplitude were related to fatigue Life as: S = 31,602 + 0,390h_s and N = 2,087 x 10^7 – 518461,803 h_s.

Acknowledgements

This research was supported by Gansu Province Major Science and Technology Special Plan Project (No.19ZD2GA002); Research on the Lifetime Design and Application Technology of Highway Concrete Bridges in Gansu Province (No.2020 05); and Gansu Provincial Science and Technology Program Project Funding (21JR7RA306).

REFERENCES

[1] Qin, A.: Research on torsion and distortion effects of single-box multi-cell composite box girder with corrugated steel webs and steel bottom plate, Lanzhou Jiaotong University, 2023, https://doi.org/10.27205/d.cnki.gltec.2023.000024.

[2] Luo, K., Ji, W., Wang, X.Y., et al.: Deflection analysis of an improved composite box girder with corrugated steel webs, Journal of Computational Mechanics, (2024), pp. 1-7, http://kns.cnki.net/kcms/ detail/21.1373.O3.20240718.1717.010.html.

[3] Zhang, H., Chen, Y., Ye, J.S., et al.: Full-range analysis of prestressed composite box girder with corrugated steel webs under pure torsion, Journal of Jilin University (Engineering Edition), (2024), pp. 1-7, https://doi.org/10.13229/j.cnki.jdxbgxb.20240546.

[4] Zhang, Z.C.: Research on bending mechanical properties and model test of steel base plate wave web-concrete combination box girder, Lanzhou Jiaotong University, 2022, https://doi.org/10.27205/d.cnki. gltec.2022.000006.

[5] Ji, W., Luo, K., Ma, W.L., et al. : Dynamic characteristics analysis and experimental study of a fabricated corrugated web steel box-concrete composite girder bridge, Journal of Vibration and Shock, 39 (2020) 20, pp. 1-7+16. https://doi.org/10.13465/ j.cnki.jvs.2020.20.001.

[6] Idiart, A.E., López, C.M., Carol, I.: Chemo-mechanical analysis of concrete cracking and degradation due to external sulfate attack: A meso-scale model, Cement and Concrete Composites, 33 (2011) 3, pp. 411-423, https://doi.org/10.1016/j.cemconcomp.2010.12.001.

[7] Kotaki, N., Ichikawa, A., Sasaki, E., et al.: A proposal of steel girder bridges with ripple web and their fatigue performance, Proceedings of the Japan Society of Civil Engineers (2004) 766, pp. 233-244, https://doi.org/10.2208/ jscej.2004.766 -233.

[8] Sugimoto, I., Murata, K., Nishida, H., et al.: Fatigue durability of joints under out-of-plane cyclic bending in corrugated steel web PC box railway bridges, Quarterly Report of RTRI, 44 (2003) 4, pp. 142-146, https://doi.org/10. 2219/rtriqr. 44.142.

[9] Wang, Z.Y., Wang, Q.Y., Chen, Y.Y., et al.: Research progress of fatigue behaviour of corrugated web girders, Journal of Highway and Transportation Research and Development, 27 (2010) 06, pp. 64-71, https://doi.org/10.3969/.issn.1008-1933.2012. 05.002.

[10] Li, L.F., Xiao, X.Y., Liu, Q.: Study on the residual flexural capacity of composite girders with corrugated steel webs after fatigue damage, China Civil Engineering Journal, 45 (2012) 7, p.9, https://doi.org/10.159 51/j. tmgcxb.2012.07.005.

[11] Dai, Y., Yuan, H., et al.: Research on fatigue property of composite girder with corrugated steel webs, (2024) 22, https://doi.org/10.25236/matmce. 2017.25.

[12] Liu, W.Z.: Experimental research on fatigue damage performance of the composite box girder with corrugated steel webs, Lanzhou Jiaotong University, (2018), https://doi.org/CNKI: CDMD:2.1018.236051.

[13] Li, P.H.: Research on fatigue test of composite girders with corrugated steel webs, Lanzhou Jiaotong University, (2018), https://doi.org/CNKI: CDMD:2.1018. 235927.

[14] Chen, P.F.: Research on fatigue damage and model test of composite girder with corrugated web and steel bottom plate, Lanzhou Jiaotong University, (2021), https://doi.org/10.27 205/d.cnki.gltec. 2021.001037.

[15] Song, S.G.: Fatigue performance analysis and model test research of composite girders with corrugated web and steel bottom, Lanzhou Jiaotong University, (2021), https://doi.org/10.27205/d.cnki. gltec.2021.000749.

[16] Huang, J., Wang M., Yang, H., et al.: Study on fatigue analysis of beam with corrugated steel webs using notch stress method, Journal of Railway Science and Engineering, 18(2021) 02, pp. 425-431, https://doi.org/10.19713/j.cnki.43-1423/u.T20200357.

[17] Wang, H., Yu, Y.T., Huang, X., et al.: Fatigue study of girder with corrugated steel web based on structural stress method, Construction Machinery, 53 (2022), pp. 56-62.

[18] Wang, G., Hi, N.X., Liu, J.X., et al.: Fatigue characteristics of composite box girder with corrugated web and steel bottom plate, Journal of Railway Engineering, 40 (2023) 07, pp. 40-45.

[19] Zhou, C.: Effect of chloride corrosion on fatigue properties of composite girder with corrugated web bottom plate and model test, Lanzhou Jiaotong University, (2023), https://doi.org/10.27205/d.cnki.gltec. 2023.001 627.

[20] Ning, X.: Fatigue damage and model test of composite girder with corrugated web plate under chloride corrosion, Lanzhou Jiaotong University, (2023), https://doi.org/10.27205/d.cnki.gltec.2023.001130.

[21] Zang, X.M.: Mechanical performance analysis and model test study of composite girder with steel bottom plate and corrugated webs under the effect of chloride salt erosion, Lanzhou Jiaotong University, (2023), https://doi.org/10.27205/d.cnki.gltec.2023.000007.

[22] JTG D64-2015: Design specification for highway steel structure bridges Beijing: China Communication Press, 2015.

[23] Yu, S.W., Feng, X.Q.: Damage mechanics, Huazhong University of Science & Technology Press (1995), ISBN:75609 10688.

[24] Ding, S., Sun, L.: Fracture mechanics, China Machine Press, (1997), ISBN:7-111-05833-X.

[25] Ouyang, Y.C.: Multiaxial fatigue life analysis of additive manufacturing titanium alloys based on Abaqus and Fe-safe, Nanchang University, (2023), https://doi.org/10.27232/d.cnki.gnchu.2023.004097.X.